Proc. Natl. Acad. Sci. USA
Vol. 95, pp. 2926–2931, March 1998
Biophysics

Long QT and ventricular arrhythmias in transgenic mice expressing the N terminus and first transmembrane segment of a voltage-gated potassium channel

BARRY LONDON[†‡], ANDREAS JERON[§¶], JUN ZHOU[§¶], PETER BUCKETT[§], XINGIANG HAN[§], GARY F. MITCHELL[§], AND GIDEON KOREN[‡§]

[†]Division of Cardiology, University of Pittsburgh Medical Center, Pittsburgh, PA 15213; and [§]Cardiovascular Division, Brigham and Women's Hospital, Harvard Medical School, Boston, MA 02115

Communicated by Eugene Braunwald, Harvard Medical School, Boston, MA, December 5, 1997 (received for review October 8, 1997)

ABSTRACT **Voltage-gated potassium channels control cardiac repolarization, and mutations of K^+ channel genes recently have been shown to cause arrhythmias and sudden death in families with the congenital long QT syndrome. The precise mechanism by which the mutations lead to QT prolongation and arrhythmias is uncertain, however. We have shown previously that an N-terminal fragment including the first transmembrane segment of the rat delayed rectifier K^+ channel Kv1.1 (*Kv1.1N206Tag*) coassembles with other K^+ channels of the Kv1 subfamily *in vitro*, inhibits the currents encoded by Kv1.5 in a dominant-negative manner when coexpressed in *Xenopus* oocytes, and traps Kv1.5 polypeptide in the endoplasmic reticulum of GH3 cells. Here we report that transgenic mice overexpressing *Kv1.1N206Tag* in the heart have a prolonged QT interval and ventricular tachycardia. Cardiac myocytes from these mice have action potential prolongation caused by a significant reduction in the density of a rapidly activating, slowly inactivating, 4-aminopyridine sensitive outward K^+ current. These changes correlate with a marked decrease in the level of Kv1.5 polypeptide. Thus, overexpression of a truncated K^+ channel in the heart alters native K^+ channel expression and has profound effects on cardiac excitability.**

Mutations of the K^+ channel genes *HERG* and *KVLQT1* cause the autosomal dominant long QT (LQT) syndrome, presumably by interfering with the cardiac currents I_{Kr} and I_{Ks} (1–6). The precise biochemical mechanism by which these mutations cause prolongation of the QT interval is uncertain. A single wild-type potassium channel gene in a heterozygous-affected individual may produce an insufficient number of functional channels to support normal repolarization of the heart. Alternatively, a mutated or truncated channel polypeptide might coassemble with wild-type channel polypeptides to produce nonfunctional channels via a dominant-negative mechanism (7).

Voltage-gated potassium channels form multimeric complexes by association of four α-subunits (8). We previously have used site-directed mutagenesis and dominant-negative techniques to study structure-function relationships and elucidate the domains that play an important role in *Shaker*-like potassium channel assembly (9–11). Overexpression of the N-terminal fragment and the first transmembrane segment of the rat brain potassium channel (*Kv1.1N206Tag*) in *Xenopus* oocytes inhibited the currents encoded by Kv1.1 and Kv1.5 in a dominant-negative manner. *Kv1.1N206Tag* also formed *in vitro* heteromultimeric complexes with Kv1.1 and Kv1.5 (11). Furthermore, we have shown that overexpression of *Kv1.1N206Tag* in GH3 cells led to the formation of heteromultimeric complexes with the native Kv1.4 and Kv1.5 potassium channel polypeptides (12). These complexes were trapped in the endoplasmic reticulum and did not reach the plasma membrane. The trapping of *Kv1.1N206Tag* led to its rapid degradation. These experiments elucidated the biochemical mechanisms that underlie the dominant-negative effect of a truncated potassium channel polypeptide overexpressed in a noncardiac mammalian cell line.

We postulated that overexpressing this truncated potassium channel in the hearts of transgenic mice would cause a substantial reduction in the outward potassium currents, presumably by trapping *Shaker*-like potassium channels in the endoplasmic reticulum. Here we report that transgenic mice overexpressing a truncated potassium channel in the heart have a prolonged QT interval and ventricular tachycardia. Cardiac myocytes from these mice have action potential prolongation caused by a significant reduction in the density of a rapidly activating, slowly inactivating, 4-aminopyridine (4-AP) sensitive outward K^+ current. These changes correlate with a marked decrease in the level of Kv1.5 polypeptide. Thus, overexpression of a truncated K^+ channel in the murine heart alters native K^+ channel expression and has profound effects on cardiac excitability.

MATERIALS AND METHODS

Transgene Construct. A cDNA fragment encoding amino acids 1–206 of rat Kv1.1 tagged at the carboxyl terminus with the hemagglutinin (HA) epitope tag (9–12) was cloned into the polycloning site of a modified pBK-CMV expression vector (Stratagene), in which the cytomegalorvirus promoter had been replaced by a 2.2-Kb fragment that contained the rat α-myosin heavy chain promoter and first two exons (13). The 3.2-Kb transgenic construct, including the simian virus 40 late polyadenylation signal, was excised from the plasmid and microinjected into fertilized oocytes derived from FVB mice at the transgenic facility of the Department of Cardiology, Children's Hospital, Boston, MA.

Membrane Preparations and Western Blots. A crude membrane fraction was isolated from the ventricles of control and transgenic mice by differential centrifugation and solubilized with 1% SDS. Equal amounts of protein (Bio-Rad) were loaded onto SDS/PAGE gels, transferred on a semidry apparatus, blocked in PBS-5% nonfat dry milk, incubated in primary antibody at 4°C overnight, washed in PBS-0.15% Tween, incubated with an horseradish peroxidase-conjugated goat anti-rabbit secondary antibody, washed, and detected by ECL (NEN).

Preparation of Isolated Myocytes. Heparinized transgenic and age-matched control FVB mice of either sex (20–30 g wt) were killed by hypercapnea. The hearts were rapidly removed and perfused in a retrograde manner at 37°C (1.5–2 ml/min) with a nominally Ca^{2+}-free solution A (containing 120 mM NaCl, 4.4

The publication costs of this article were defrayed in part by page charge payment. This article must therefore be hereby marked "*advertisement*" in accordance with 18 U.S.C. §1734 solely to indicate this fact.

Abbreviations: LQT, long QT; HA, hemagglutinin; ECG, electrocardiogram; APD, action potential duration; 4-AP, 4-aminopyridine; QTc, corrected QT; QT_o, observed QT.

[‡]To whom reprint requests should be addressed. e-mail: koren@calvin.bwh.harvard.edu or London@card2.cath.upmc.edu.
[¶]A.J. and J.Z. contributed equally to this work.

mM KCl, 1.0 mM $MgCl_2$, 18 mM $NaCO_3$, 11 mM glucose, 20 mM 2,3-butanedione monoxime, 4 mM Hepes, and 0.13 units/ml insulin) for 5–7 min, followed by 8–15 min with enzyme I solution [solution A with 0.25 mg/ml collagenase (type I, Worthington), 0.2 mg/ml hyaluronidase (type II, Sigma), and 1 mg/ml fatty acid-free BSA]. After perfusion, the ventricles were chopped into small pieces, incubated at 37°C in enzyme II solution [enzyme I + 0.8 μg/ml protease (type IXV, Sigma) and 0.5 mM Ca^{2+})] for 10 min, and mechanically dispersed with a 10-ml disposable pipette. After repeatedly washing by a series of centrifugations and resuspensions in a medium containing 50% buffer A and 50% DMEM (GIBCO/BRL) supplemented with antibiotics (penicillin/streptomycin) and 5–10% fetal calf serum, cells were plated on glass coverslips coated with laminin (Collaborative Research) and maintained at 37°C in an air/CO_2 (95:5) environment. Calcium-tolerant, rod-shaped ventricular myocytes with clear striations were selected randomly and used for the electrophysiological studies on the day of isolation.

Cell Radiolabeling and Immunoprecipitation. Cardiocytes were labeled for 16 hr with 0.1 mCi/ml of Translabel (ICN) in methionine- and cysteine-free DMEM. Cells were lysed in 50 mM Tris, pH 8/0.1% SDS/1% Nonidet P-40/0.5% deoxycholate/150 mM NaCl (RIPA buffer) containing a mixture of protease inhibitors, and were centrifuged at 3,000 rpm for 10 min. Cell extracts were precleared with protein A Sepharose for 1 hr and incubated for 1 hr with the indicated antibodies. Immunocomplexes were collected with protein A Sepharose and electrophoresed in an 11%-polyacrylamide/SDS gel.

Monitoring Studies. Mice tested ranged in age from 3 to 6 months. Data were acquired by using a Data Sciences implantable radio frequency transmitter (TA 10EA-F20) and a receiver placed under each cage. The transmitter was implanted in a subcutaneous pocket along the spine. The cathodal lead was placed over the scapula, and the anodal lead was placed on the chest wall near the apex of the heart. The analog electrocardiogram (ECG) signal was digitized at 500 Hz by using a 16-bit analog to digital converter (model AT-MIO-16XE-10, National Instruments, Austin, TX) in a personal computer. By using custom software, continuous digital recordings were acquired and stored on CD-ROM. The QT interval of the signal-averaged complex was determined manually by placing cursors on the beginning of the QRS signal and the end of the T-wave. Comparison of simultaneous recordings of surface ECG under ketamine anesthesia (lead I, II, and III) and transmitter ECG revealed minimal differences in the observed QT interval (<3%, $n = 7$, P = not significant). Arrhythmias were detected based on rate criteria by screening of the stored digital recordings for sudden changes in individual RR intervals. Eleven control and 12 LQT mice were monitored for 48 hr after surgery for arrhythmia detection. Seven control and nine LQT mice were monitored for an additional 48 hr. All ECG data were expressed as mean ± SD. Student's t test was used to compare unpaired data between two groups, and two-tailed $P < 0.05$ was taken to indicate statistical significance. ANOVA for repeated measurements was used to analyze the effect of ketamine.

Electrophysiological Studies. Whole-cell configuration of patch-clamp technique was used to record K^+ currents and action potentials. Glass capillaries (World Precision Instruments, Sarasota, FL) were pulled with a horizontal pipette puller (model P-87, Sutter Instruments, Novato, CA) and had resistances of 1.5–6 MΩ when filled with a standard pipette solution containing 137 mM KCl, 1 mM $MgCl_2$, 0.5 mM $CaCl_2$, 10 mM Hepes, 5 mM EGTA, 5 mM Mg_2ATP, 5 mM Na-creatine phosphate, and 0.5 mM GTP·tris, pH 7.2 with KOH. The electrodes were connected to an Axopatch 200A amplifier, and a DigiData 1200 interface controlled by pClamp 6.0.4 software was used for generating command pulses and data acquisition (Axon Instruments, Foster City, CA). After formation of a "gigaohm" seal between the recording electrode and the myocyte membrane, electrode capacitance was fully compensated. In the whole-cell configuration, series resistance and cell capacitance were routinely compensated and, consequently, the capacitative transient decayed completely to baseline in all cells within 3.0 ms. Cells were superfused at 1–2 ml/min with Tyrode's solution containing 137 mM NaCl, 5.4 mM KCl, 1 mM $MgCl_2$, 1 mM $CaCl_2$, 10 mM glucose, and 10 mM Hepes, pH 7.4 with NaOH. Action potentials were recorded in current-clamp mode in normal Tyrode's solution by injecting suprathreshold current pulses through the patch-clamp electrode. To record the depolarization-activated K currents, 2 mM $CoCl_2$ was used to inhibit I_{Ca}. Mg_2ATP in the pipettes would suppress the ATP-sensitive potassium current. All the recordings were done after 5 min of membrane rupture at room temperature (22–24°C). The time constants for inactivation were determined by least-square fitting of a double exponential function $y(t) = A_1{*}EXP(-t/\tau_1) + A_2{*}EXP(-t/\tau_2) + A_0$ to current traces, where τ_1 and τ_2 represents the fast and slow time constants of inactivation, respectively. Data were expressed as mean ± SEM. Student's t test was used to compare unpaired data between two groups, and two-tailed $P < 0.05$ was taken to indicate statistical significance.

RESULTS

We generated seven founder mice by using a transgenic construct that includes the rat α-myosin heavy chain promoter (13), a cDNA fragment that encodes the N terminus and the first transmembrane segment of the rat brain K^+ channel Kv1.1 tagged with an HA epitope (*Kv1.1N206Tag*) (9, 11–12), and the simian virus 40 poly(A) tail (Fig. 1 *a* and *b*). Northern blot analysis using a probe from the 5′ end of Kv1.1 demonstrated expression of the ≈900-bp *Kv1.1N206Tag* transcript in three of the lines (Fig. 1*c*, *Left*). Native channel expression (>8 KB transcript) was detected only in the brain, whereas expression of the transgene was abundant in only the heart (Fig. 1*c*, *Right*). Western blot analysis using an antibody to the HA epitope revealed a 25-kDa polypeptide expressed in the hearts of LQT mice (line B102) and absent in control mice (Fig. 1*d*). Similarly, immunoprecipitation of metabolically labeled rod-shaped cardiac myocytes isolated from LQT mice and of metabolically labeled GH3 cells stably transfected with *Kv1.1N206Tag* (GHT69 cells) demonstrated a polypeptide of the same size that was not present in control myocytes or in GHT69 cells incubated with an excess of HA peptide during the immunoprecipitation (Fig. 1*e*). Histological studies of the heart did not reveal significant differences between LQT and control mice (data not shown).

To determine whether expression of the transgene in the heart of these animals modulates the phenotype, we characterized their surface ECGs. Under ketamine anesthesia, F_1 heterozygote mice from the three lines that expressed the *Kv1.1N206Tag* transcript had corrected QT intervals (QTc, see below) that were 116% (B112), 122% (B114), and 167% (B102) of the mean QTc interval of the three transgenic F_1 mice from lines that did not express *Kv1.1N206Tag* transcript (Fig. 1*c*). We further characterized the ECGs of conscious mice derived from line B102 by using high-quality continuous recording via an implantable telemetry system (Datasciences, Minneapolis) (14). The mean QT interval of the LQT mice was 59.9 ± 2.5 ms compared with 54.2 ± 1.8 ms in age- and sex-matched littermate controls ($n = 10$ each group, $P < .01$), whereas the mean RR interval was 99 ± 8 ms in LQT mice vs. 97 ± 11 ms in controls (not significant). As expected, the observed QT interval correlated with cycle length, but the difference between the control and LQT mice was present over a wide range of rates and during both day and night (Fig. 2*a*). Anesthesia with ketamine (50 mg/kg), a known blocker of Na^+ and K^+ channels (15–17), resulted in excessive prolongation of the QT interval in transgenic mice compared with controls at similar heart rate (Fig. 2 *b* and *c*), with a mean QT interval of 135 ± 29 ms in LQT mice compared with 99 ± 11 ms in controls ($n = 20$ each group, $P < 0.001$) and an RR interval of 299 ± 101 ms in LQT mice vs. 265 ± 69 ms in controls (not significant). To directly compare the observed QT interval (QT_o) at different

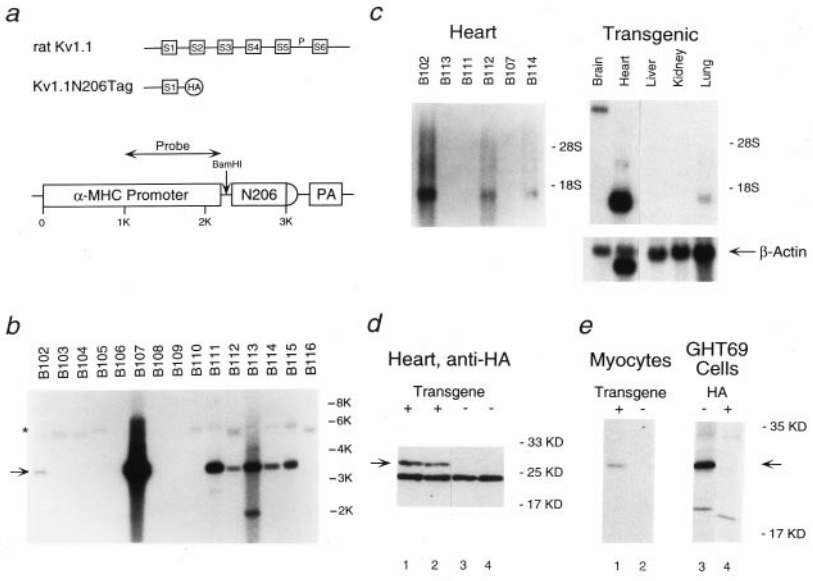

FIG. 1. Expression of the N-terminal fragment of rat Kv1.1 in the hearts of transgenic mice. (*a*) Schematic representation of rat brain potassium channel Kv1.1 (*Top*), the N-terminal fragment *Kv1.1N206Tag* (*Middle*), and the transgenic construct (*Bottom*). HA represents the HA epitope added to the N-terminal fragment of Kv1.1. The α-myosin heavy chain contained ≈1 KB of the promoter followed by exon 1, the first intron, and part of exon 2 (5′ untranslated). N206 represents the N-terminal fragment *Kv1.1N206Tag* and PA represents the polyadenylation signal. (*b*) Genomic Southern blot of tail DNA isolated from 16 F_o mice, digested with *Bam*HI, and probed with the fragment of the α-myosin heavy chain denoted in *a*. The native mouse α-myosin heavy chain gene (*) and the transgene (arrow) are indicated. Note that each of the seven transgenic founders have multiple copies of the transgene. (*c*) Northern blot analysis of 2 μg of poly(A)$^+$ RNA (PolyATract, Promega) from the hearts of F_1 mice from the lines indicated (*Left*) and of 15 μg of total RNA (RNEasy, Qiagen) from the indicated organs of an F_1 mouse of the B102 line (*Right*), probed with the N-terminal fragment of Kv1.1. Relative loading of RNA was confirmed by reprobing with a 700-bp fragment of the β-actin gene. (*d*) Western blot analysis of the steady-state levels of *Kv1.1N206Tag* polypeptide present in the membrane fraction of LQT hearts (lanes 1–2) and control hearts (lanes 3–4) using a rabbit polyclonal antibody directed against the HA epitope (Santa Cruz Biotechnology). The arrow indicates the position of *Kv1.1N206Tag*. (*e*) Immunoprecipitation analysis of *Kv1.1N206Tag* expressed in primary culture of adult mouse rod shape cardiocytes derived from two LQT mice (lane 1), control cardiocytes (lane 2), and GH3 cells stably transfected with *Kv1.1N206Tag* (GHT69) (lane 3). In lane 4, the immunoprecipitation was blocked with 90 nmols of HA peptide. Total cell lysates were immunoprecipitated with anti-HA antibody (12CA5). The pellets were analyzed on SDS/PAGE. The arrow indicates the position of *Kv1.1N206Tag*.

heart rates, we developed a correction formula: $QTc = QT_o/(RR_o/100)^{1/2}$ where the QTc is the corrected QT interval (14). Ketamine induced an excessive prolongation of the mean QTc interval measured in the first 2 hr after drug administration in LQT mice (Fig. 2*d*). The QTc was increased from 59.7 ± 2.0 to 71.2 ± 7.0 ms in LQT mice ($P < 0.001$; $n = 9$) compared with minimal prolongation in control animals (from 54.5 ± 1.2 ms to 56.9 ± 2.8 ms; not significant; $n = 7$). To determine whether the difference was dependent on age we compared the peak QTc interval obtained from surface ECG under ketamine anesthesia of LQT mice older than 6 months to that of control mice (range in 6–10 months). The QTc interval of LQT mice was 79 ± 13 ms ($n = 10$) compared with 61 ± 9 ($n = 10$) ms for the control mice ($P < 0.005$). Thus, age had no effect on the dominant negative effect of the transgene as reflected by the extent of prolongation of the QT interval under ketamine anesthesia.

We detected an increased frequency of ventricular premature beats in LQT mice (11.6 ± 14.4 per day, $n = 10$) compared with controls (1.3 ± 0.9 per day; $n = 12$; $P = 0.03$). Complex ventricular arrhythmias such as couplets were recorded in all LQT mice monitored, but in none of the control mice. Spontaneous self-terminating episodes of tachyarrhythmias characterized by fusions beats, wider QRS complexes with a different morphology and atrio-ventricular dissociation also were detected in seven of the 12 LQT mice but in none of the control mice (Fig. 2*e*). These arrhythmias likely represent nonsustained ventricular tachycardia although we cannot exclude junctional tachycardia with retrograde atrio-ventricular block and aberrant conduction. LQT mice were followed for up to 2 years with no significant increase in spontaneous sudden death.

We then characterized the electrophysiological properties of cardiac myocytes derived from LQT mice. The action potential duration (APD) was significantly longer in LQT myocytes than in controls (Fig. 3*a*). APD_{30}, APD_{50}, and APD_{95} were 5.4 ± 0.4, 9.6 ± 1.0, and 82.5 ± 6.7 ms, respectively, in LQT cells ($n = 12$) compared with 3.4 ± 0.2, 4.7 ± 0.3, and 38.8 ± 2.7 ms in control cells ($n = 21$; $P < 0.001$ for each set). The resting membrane potential and action potential amplitude were similar in both groups (−70.0 ± 0.5 and 112.1 ± 2.9 mV, in LQT myocytes versus −70.3 ± 0.3 and 104.0 ± 3.9 mV, respectively, in controls). We next studied outward K^+ currents by using the whole-cell voltage clamp method. Depolarizing steps produced outward currents that rose rapidly to a peak and decayed (Fig. 3*b*). A noninactivating component (I_{sus}) remained despite depolarizations as long as 3.5 sec (data not shown). There was no significant difference between control and LQT myocytes in the density of the transient outward currents (I_{to}) as reflected by the difference between the peak current and the current level at the end of the 250-ms test pulses. The density of the remaining late outward current was significantly decreased at potentials positive to −20 mV in LQT myocytes ($n = 15$) compared with controls ($n = 24$, $P < 0.05$) (Fig. 3*b*), however, without a significant shift in the voltage dependence of the current. The inactivation kinetics of currents elicited were well fit by using a biexponential function. At 60 mV, the fast time constant (τ_{fast}) was 33.5 ± 2.0 ms and the slow time constant (τ_{slow}) was 595 ± 29.3 ms ($n = 7$). In contrast, the inactivation kinetics for seven of 15 LQT myocytes were well fit by using a single exponential and had a time constants similar to τ_{fast} (37.8 ± 1.7 ms at 60 ms).

To further define I_{slow}, we inactivated I_{to} by using a 200-ms depolarizing prepulse (Fig. 3*c*). This protocol elicited a rapidly activating current ($\tau = 2.4 \pm 0.3$ ms at 50 mV) with slow inactivation (I_{slow}) and an associated deactivating tail current (I_{tail}) that was prominent in control myocytes but either absent or significantly reduced in LQT myocytes as evident by a significant reduction in the density of I_{tail} (2.8 ± 0.2 pA per pF, $n = 7$, in control myocytes compared with 1.8 ± 0.2 pA per pF, $n = 6$ in LQT myocytes, $P < 0.01$) (Fig. 3 *c* and *d*). The marked reduction in the density of I_{tail} in LQT myocytes could not be accounted for by a shift in voltage sensitivity of I_{slow} (Fig. 3*b*). We next tested the sensitivity of I_{to} and I_{slow} to 4-AP. Fitting the dose-response curves of 4-AP to I_{slow} of each control cell gave an IC_{50} value of 32.1 ± 5.2 μM ($n = 9$). Indeed, 4-AP could inhibit I_{slow} and I_{tail} in control myocytes to a larger extent than in LQT myocytes (Fig. 3 *c* and *d*). By contrast, the IC_{50} of I_{to} for 4-AP was 215.8 ± 66.3 in control ($n = 8$) and 296.1 ± 36.8 μM in LQT myocytes ($n = 5$, $P > 0.05$). Because I_{slow} is almost abolished in LQT cardiocytes, it is likely that current remaining is primarily I_{sus}. Indeed, the 4-AP-resistant I_{tail} in control cardiocytes did not differ from that of LQT cardiocytes (Fig. 3*d*), suggesting that I_{sus} was not altered. Fig. 4 *a–c* illustrates the component of the outward K^+ current sensitive

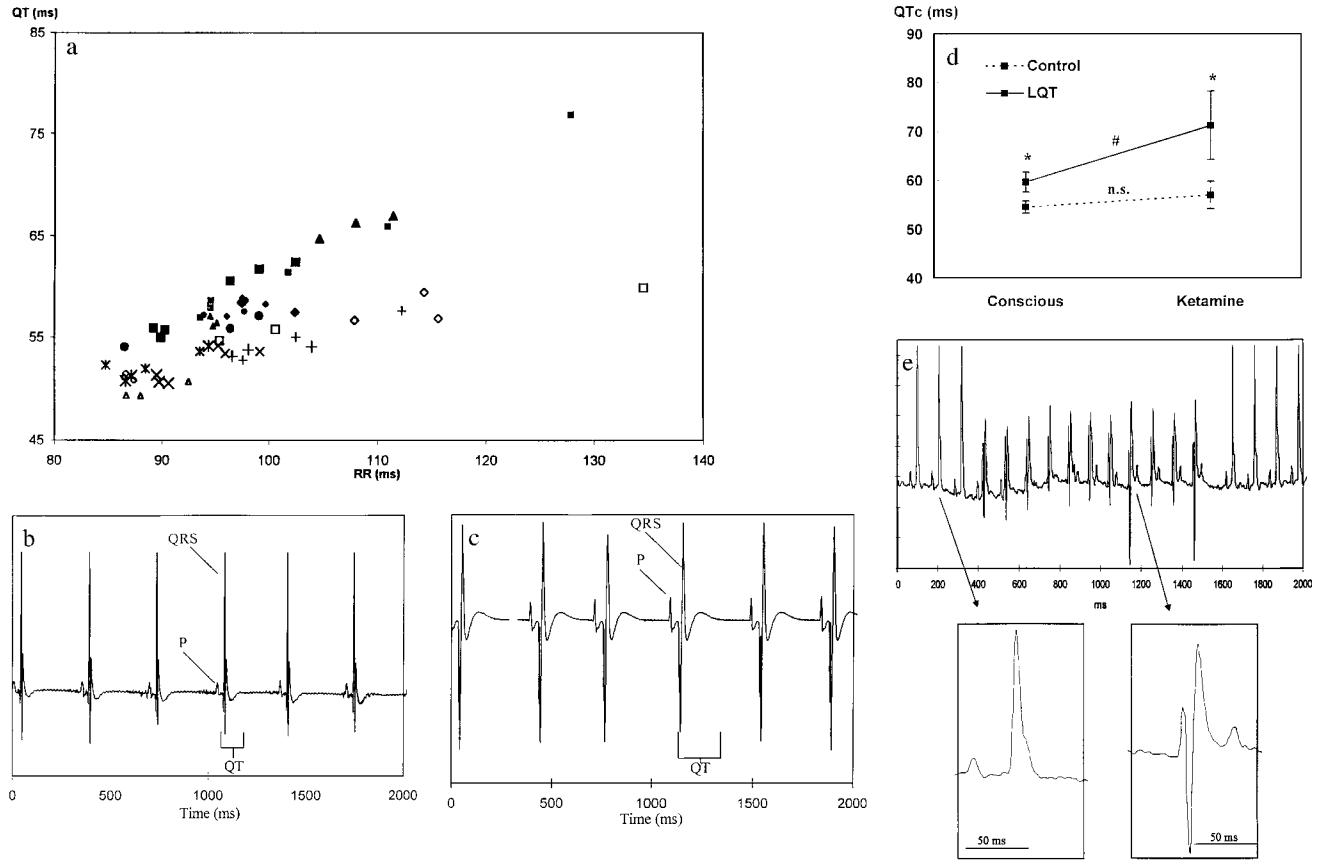

FIG. 2. Analysis of the rhythm and QT intervals of ECGs obtained from LQT and control mice. (*a*) The relationships between the observed QT interval and the RR intervals in the conscious LQT mice (◆, ●, and ▲, $n = 10$) and control mice (△, ◇, ×, +, $n = 10$). Each point represents an average of 72 measurements of the QT and RR intervals (every 20 min) per 24 hr. Each measurement is an average of a 4-sec screen. Each mouse was monitored continuously for 3 days and is therefore represented by three points. (*b*) The ECG of an anesthetized 3-month-old control mouse (50 mg/kg ketamine and 10 mg/kg xylazine) recorded by the transmitter. The observed heart rate was 180 beats per minute (bpm), and the observed QT interval was 101 ms. (*c*) The ECG of an anesthetized matched LQT mouse (50 mg/kg ketamine and 10 mg/kg xylazine) recorded by the transmitter. The observed heart rate was 180 bpm, and the observed QT interval was 179 ms. (*d*) Sensitivity of the QTc interval of LQT mice to ketamine. The average QTc interval of anesthetized and conscious LQT and control mice (average of 2 hr after 50 mg/kg ketamine administration). The ketamine-induced prolongation of the QTc interval in LQT mice was significantly greater than that of control. (*e*) Surface ECG recording of an 11-beat run of ventricular tachycardia in a conscious freely moving LQT mouse. Note the atrio-ventricular dissociation. The enlarged QRS complexes demonstrate that the individual QRS complexes in the nonsustained ventricular tachycardia differ substantially from the sinus QRS complexes. The sinus heart rate is about 530 bpm (RR interval of 113 ms). The rate of the ventricular tachycardia is 570 bpm (RR interval of 105 ms).

to 50 μM 4-AP. In control myocytes, this current was characterized by a slow inactivation that could be well fitted by a single exponential function with a time constant of 597.4 ± 42.0 ms ($n = 5$) at 60 mV, similar to τ_{slow}. This component was significantly reduced or absent in LQT myocytes. α-Dendrotoxin (14.3 nM, a blocker of Kv1.1 and Kv1.2) (18) and E-4031 (1 μM, a specific blocker of I_{Kr}), did not exert significant effects on the outward potassium currents in both groups of myocytes (data not shown).

Collectively, these results indicate that *Kv1.1N206Tag* primarily targets a highly 4-AP sensitive component of the outward K^+ current with rapid activation and slow inactivation kinetics. I_{slow} has an IC_{50} for 4-AP similar to that of Kv1.5 expressed in *Xenopus* oocytes or mammalian cells (18). We therefore compared the steady-state level of Kv1.5 subunit polypeptide in crude membrane preparations from the ventricles of control and LQT mice. Kv1.5 was markedly reduced in LQT ventricular muscle compared with control (Fig. 4*d*). These studies provide strong evidence that I_{slow} in mouse ventricular myocytes is encoded at least in part by the Kv1.5 gene.

DISCUSSION

Previous studies in neonatal and adult mouse cardiomyocytes have documented the presence of cardiac potassium currents, including I_{to}, IK_s, I_{Kr}, and I_{sus} (19–22). We have shown that a dominant-negative approach targeting Shaker-like potassium channels decreases Kv1.5 protein and eliminates a slowly inactivating 4-AP sensitive current, I_{slow}, that formerly was included as a part of Ito (19). The IC_{50} of I_{slow}, <50 μM, is similar to that of channels encoded by Kv1.5 expressed in *Xenopus* oocytes or mammalian cell lines (18). Channels encoded by Kv4.2 or 4.3 have a higher IC_{50} (300 μM) that is similar to that of Ito (18). Kv1.4 protein is not abundant in the mouse heart, and targeted disruption of Kv1.4 in the mouse does not decrease inactivating currents (23). Thus, although we cannot completely exclude up-regulation or down-regulation of additional channels, our results provide strong evidence that Kv1.5 underlies I_{slow} in the mouse ventricle.

Ketamine anesthesia enhances the prolongation of QTc in the dominant negative LQT compared with controls. Ketamine inhibits several cardiac potassium currents, including I_{to}, I_{K1}, and I_{KATP} (15–17), increases sympathetic nerve activity (24), and prolongs APD in the rat heart (15, 17). We speculate that the loss of the potassium current I_{slow} in the LQT mice leaves them more vulnerable to QT prolongation by blockade of other potassium currents by anesthetic agents such as ketamine.

Homomeric Kv1.5 cDNA expressed in *Xenopus* oocytes produces noninactivating 4-AP sensitive outward K^+ currents

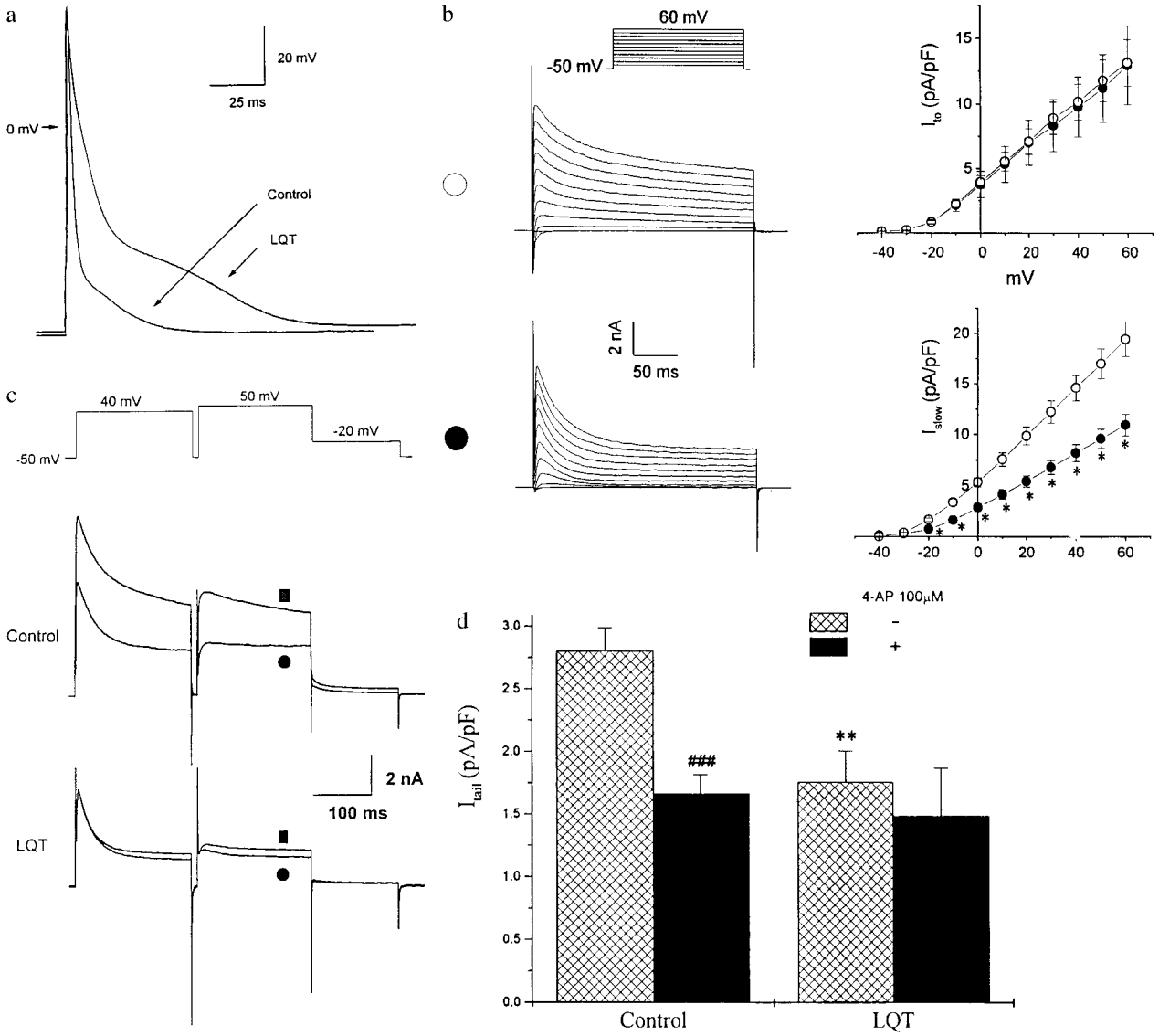

FIG. 3. Characterization of AP and the outward potassium currents in LQT cardiocytes. (*a*) Transmembrane AP recorded from a representative control and a LQT mouse cardiocyte. APs were elicited by suprathreshold current injected through the electrode at 0.5 Hz. For better superimposition, stimulatory artifacts resulting from current injection were minimized off-line. (*b*) Voltage-dependent K^+ current traces and current-voltage relationships in control (*; $n = 24$) and LQT mouse ventricular myocytes (●; $n = 16$). Traces from representative cells are shown (*Left*). Current density was obtained by normalizing the current amplitude to cell capacitance. The currents were elicited by 10 mV step depolarizations between −40 to +60 mV from −50 mV holding potential. I_{to} was defined as the difference between the peak outward current and the current level at the end of the 250-ms pulse. The current remaining after 250 ms was significantly lower in LQT myocytes ($P < 0.05$). (*c*) Effects of 50 μM 4-AP on the outward currents of a representative ventricular myocyte derived from either a control or a matched LQT mouse. The voltage protocol is shown (*Top*). ■ and ● indicate the current traces before and after application of 4-AP respectively. (*d*) Summary of the effects of 100 μM 4-AP on I_{tail} of control and LQT myocytes. I_{tail} was defined as the difference between the peak and the current at the end of −20-mV pulse. The density of I_{tail} was significantly larger in control cardiocytes compared with LQT (**, $P < 0.01$). 4-AP abolished over 40% of I_{tail} in control cardiocytes (###, $P < 0.001$), but had no significant effect in LQT cardiocytes.

(18, 25). I_{Kur}, a rapidly activating 4-AP sensitive noninactivating human atrial K^+ current, is thought to be encoded by hKv1.5 (26). In GH3 cells Kv1.5 contributes to both a noninactivating outward K^+ current and to a current with inactivation kinetics that are faster than those of I_{Kur} and I_{slow} (27, 28). The diversity of the inactivation properties of these currents and I_{slow}, all of which are thought to be coded by Kv1.5, is likely caused by coassembly with other K^+ channel subunits (25, 29, 30) or interactions with a β subunits such as β_3 (31, 32).

Proper assembly of K^+ channel complexes requires interactions between four subunits (8), the specificity of which is determined by a domain located at the N terminus (11, 33–35). Overexpression of *Kv1.1N206Tag* in *Xenopus* oocytes abolishes expression of Kv1.5 encoded outward currents, and in GH3 cells it results in the trapping of Kv1.5 polypeptides in the endoplasmic reticulum (11, 12). Here we observed a marked decrease in the steady-state levels of Kv1.5 polypeptide that correlates with a marked reduction in the density of I_{slow}. It therefore is likely that the dominant-negative effect of overexpression of *Kv1.1N206Tag* in the mouse heart is mediated by the trapping of native *Kv1.1N206Tag* − Kv1.5 complexes in the endoplasmic reticulum, causing increased degradation of Kv1.5 polypeptide. We propose that our observations in LQT mice and GH3 cells may explain the dominant-negative effect of mutations in the first transmembrane segment of Kv1.1 that cause episodic ataxia (36). We speculate that dominant-negative effect of a deletion mutation of *HERG* that truncates the channel polypeptide after S1 and causes LQT syndrome also may result from interference with the proper assembly of these channels (7, 37).

Kv1.1N206Tag may have been expressed in atrial cells as well as ventricular cells. Although we did not study the electrophysiology of atrial cells, we did not observe a change in heart

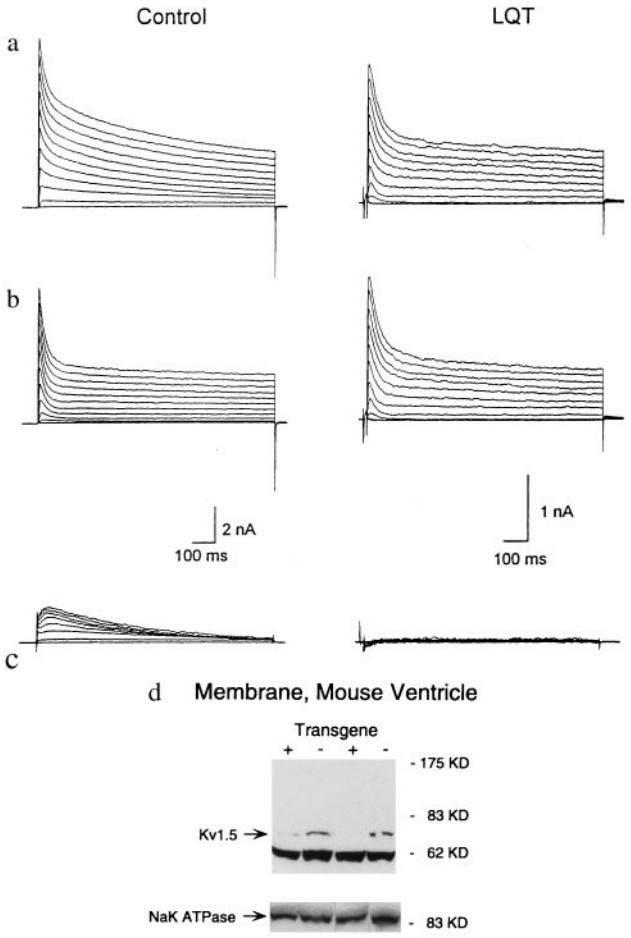

FIG. 4. Effect of 4-AP on outward K^+ currents. (*a–c*) Examples of outward K^+ currents recorded from mouse cardiocytes derived from control and LQT mice before (*a*) and after (*b*) application of 50 μM 4-AP. *c* illustrates the 4-AP-sensitive components obtained by the subtraction of the currents in *b* from the currents in ***aa***. A series of prolonged (1,000 ms) test pulses were applied to elicit the outward currents. (*d*) Western blot analysis of the steady-state levels of Kv1.5 in membrane preparations from the hearts of LQT mice and nontransgenic littermate controls, using a rabbit polyclonal antibody directed against Kv1.5 (Upstate Biotechnology). A gel loaded with the same amount of membrane extract (not boiled) and incubated with an antibody directed against the α subunit of the rat Na-K ATPase demonstrated equal loading of membrane extracts, as did another gel stained with Coumassie blue (data not shown). Similar results were obtained for three transgenic and three control mice, and the blot was repeated in triplicate.

rate, prolongation of the PR interval, or an increase in the frequency of supraventricular arrhythmias.

We observed an increase in the frequency of ventricular premature beats and spontaneous episodes of ventricular tachycardia during ambulatory telemetry monitoring of the LQT mice. Both *in vitro* and *in vivo* studies correlate APD prolongation with the development of early afterdepolarizations (EADs), or oscillations in the repolarization phase of the action potential (38). EADs can trigger action potentials and, when propagated in the heart, give rise to ventricular premature beats. This triggered activity may initiate a reentrant arrhythmia and lead to ventricular tachycardia in the mice. Thus, although mouse and human cardiac electrophysiology differ substantially, further study of the LQT mouse model may shed light on the relationship between prolongation of the QT interval and the genesis of ventricular tachyarrhythmias.

We thank S. Schieferl for technical assistance. We wish to thank Dr. M. C. Sanguinetti for E-4031. This work was supported in part by the National Heart, Lung, and Blood Institute (B.L., G.F.M., and G.K.), a Child Health Research Grant from the Charles H. Hood Foundation (B.L.), an American Heart Association Established Investigator Award (G.K.), and a Deutsche Forschungsgemeinschaft Fellowship Award (A.J.).

1. Curran, M. E., Splawski, I., Timothy, K. W., Vincent, G. M., Green, E. D. & Keating, M. T. (1995) *Cell* **80,** 795–803.
2. Wang, Q., Curran, M. E., Splawski, I., Burn, T. C., Millholland, J. M., Van Raay, T. J., Shen, J., Timothy, K. W., Vincent, G. M., de Jager, T., *et al.* (1996) *Nat. Genet.* **12,** 17–23.
3. Sanguinetti, M. C., Jiang, C., Curran, M. E. & Keating, M. T. (1995) *Cell* **81,** 299–307.
4. Trudeau, M. C., Waronhe, J. M., Ganetsky, B. & Robertson, G. A. (1995) *Science* **269,** 92–95.
5. Sanguinetti, M. C., Curran, M. E., Zou, A., Shen, J., Spector, P. S., Atkinson, D. L. & Keating, M. T. (1996) *Nature (London)* **384,** 80–83.
6. Barhanin, J., Lesage, F., Guillemare, E., Fink, M., Lazdunski, M. & Romey, G. (1996) *Nature (London)* **384,** 78–80.
7. Sanguinetti, M. C., Curran, M. E., Spector, P. S. & Keating, M. T. (1996) *Proc. Natl. Acad. Sci. USA* **93,** 2208–2212.
8. MacKinnon, R. (1991) *Nature (London)* **350,** 232–235.
9. Koren, G., Liman, E. R., Logothetis, D. E., Nadal-Ginard, B. & Hess, P. (1990) *Neuron* **4,** 39–52.
10. Liman, E. R., Hess, P., Weaver, F. W. & Koren, G. (1991) *Nature (London)* **353,** 752–756.
11. Babila, T., Moscucci, A., Wang, H., Weaver, F. E. & Koren, G. (1994) *Neuron* **12,** 615–626.
12. Folco, E., Mathur, R., Mori, Y., Buckett, P. & Koren, G. (1997) *J. Biol. Chem.* **272,** 26505–26510.
13. Mahdavi, V., Koren, G., Michaud, S., Pinset, C. & Izumo, S. (1998) *UCLA Symposia on Molecular and Cellular Biology, New Series*, eds. Stockdale, F. and Kedes, L. (Liss, New York), pp. 369–379.
14. Mitchell, G. F., Jeron, A. & Koren, G. (1998) *Heart Circ. Physiol.* **43,** H747–H751.
15. Endow, M., Hattori, Y., Nakaya, H., Gotoh, Y. & Kanno, M. (1992) *Anesthesiology* **76,** 409–418.
16. Baum, V. C. (1993) *Anesth. Analg.* **76,** 18–23.
17. Ko, S.-H., Lee, S.-K., Han, Y.-J., Choe, H., Kwak, Y.-G., Chae, S.-W., Cho, K.-P. & Song, H.-S. (1997) *Anesthesiology* **87,** 68–74.
18. Chandy, K. G. & Gutman, G. A., Noth, R. A. (1995) *Handbook of Receptors and Channels: Ligand and Voltage-Gated Ion Channels* (CRC, Boca Raton, FL), pp. 43–45.
19. Wang, L. & Duff, H. J. (1997) *Circ. Res.* **81,** 120–127.
20. Wang, L. & Duff, H. J. (1996) *Am. J. Physiol.* **270,** H2088–H2093.
21. Nuss, B. H. & Marban, E. (1994) *J. Physiol.* **479,** 265–279.
22. Benndorf, K., Markwardt, F. & Nilius, B. (1987) *Pflügers Arch.* **409,** 641–643.
23. London, B., Wang, D. W., Hill, J. A., Bennett, P. B. & Fishman, M. C. (1997) *Circulation* **96,** 422 (Abstr.).
24. Okamoto, H., Hoka, S., Kawasake, T., Okuyama, T. & Takahashi, S. (1994) *Anesthesiology* **81,** 137–146.
25. Matsubara, H., Liman, E. R., Hess, P. & Koren, G. (1991) *J. Biol. Chem.* **266,** 13324–13328.
26. Wang, Z., Fermini, B. & Nattel, S. (1993) *Circ. Res.* **73,** 1061–1076.
27. Takimoto, K., Fomina, A. F., Gealy, R., Trimmer, J. S. & Levitan, E. S. (1993) *Neuron* **11,** 359–369.
28. Chung, S., Saal, D. B. & Kaczmarek, L. K. (1995) *Proc. Natl. Acad. Sci. USA* **92,** 5955–5959.
29. Isacoff, E. Y., Jan, Y. N. & Jan, L. Y. (1990) *Nature (London)* **345,** 530–534.
30. Ruppefsberg, P., Schroter, K. H., Sakmann, R., Stocker, M., Sewing, S. & Pongs, O. (1990) *Nature (London)* **345,** 535–537.
31. Rettig, J., Heinemann, S. H., Wunder, F., Lorra, C., Parcej, D. N., Dolly, J. O. & Pongs, O. (1994) *Nature (London)* **369,** 289–294.
32. Morales, M. J., Castellino, R. C., Crews, A. L., Rasmusson, R. L. & Strauss, H. C. (1995) *J. Biol. Chem.* **270,** 6272–6277.
33. Li, M., Jan, Y. N. & Jan, L. Y. (1992) *Science* **257,** 1225–1230.
34. Shen, N. V., Chen, X., Boyer, M. M. & Pfaffinger, P. J. (1993) *Neuron* **11,** 67–76.
35. Tu, L., Santarelli, V. & Deutsch, C. (1995) *Biophys. J.* **68,** 147–156.
36. Adelman, J. P., Bond, C. T., Pessia, M. & Maylie J. (1995) *Neuron* **15,** 1449–1554.
37. Li, X., Xu, J. & Li, M. (1997) *J. Biol. Chem.* **272,** 705–708.
38. Roden, D. M., Lazzara, R., Rosen, M., Schwartz, P. J., Towbin, J. & Vincent, G. M. (1996) *Circulation* **94,** 1996–2012.